Influence of small-molecule material on performance of polymer solar cells based on MEH-PPV:PCBM blend*

Liu Xiao-Dong(刘晓东), Xu Zheng(徐 征)†, Zhang Fu-Jun(张福俊)‡,
Zhao Su-Ling(赵谡玲), Zhang Tian-Hui(张天慧), Gong Wei(龚 伟),
Song Jing-Lu (宋晶路), Kong Chao(孔 超), Yan Guang(闫 光), and Xu Xu-Rong(徐叙瑢)

Key Laboratory of Luminescence and Optical Information, Beijing Jiaotong University, Ministry of Education, Beijing 100044, *China*

(Received 12 April 2010; revised manuscript received 21 May 2010)

In this work, the influence of a small-molecule material, tris(8-hydroxyquinoline) aluminum (Alq_3), on bulk heterojunction (BHJ) polymer solar cells (PSCs) is investigated in devices based on the blend of poly(2-methoxy-5-(2-ethylhexyloxy)-1,4-phenylenevinylene) (MEH-PPV) and [6,6]-phenyl-C_{61}-butyric acid methyl ester (PCBM). By doping Alq_3 into MEH-PPV:PCBM solution, the number of MEH-PPV excitons can be effectively increased due to the energy transfer from Alq_3 to MEH-PPV, which probably induces the increase of photocurrent generated by excitons dissociation. However, the low carrier mobility of Alq_3 is detrimental to the efficient charge transport, thereby blocking the charge collection by the respective electrodes. The balance between photon absorption and charge transport in the active layer plays a key role in the performance of PSCs. For the case of 5 wt.% Alq_3 doping, the device performance is deteriorated rather than improved as compared with that of the undoped device. On the other hand, we adopt Alq_3 as a buffer layer instead of commonly used LiF. All the photovoltaic parameters are improved, yielding an 80% increase in power conversion efficiency (PCE) at the optimum thickness (1 nm) as compared with that of the device without any buffer layer. Even for the 5 wt.% Alq_3 doped device, the PCE has a slight enhancement compared with that of the standard device after modification with 1 nm (or 2 nm) thermally evaporated Alq_3. The performance deterioration of Alq_3-doped devices can be explained by the low solubility of Alq_3, which probably deteriorates the bicontinuous D–A network morphology; while the performance improvement of the devices with Alq_3 as a buffer layer is attributed to the increased light harvesting, as well as blocking the hole leakage from MEH-PPV to the aluminum (Al) electrode due to the lower highest occupied molecular orbital (HOMO) level of Alq_3 compared with that of MEH-PPV.

Keywords: bulk heterojunction polymer solar cells, Alq_3, doping, buffer layer
PACC: 8630J, 7360T, 7340

1. Introduction

Organic solar cells have attracted more attention due to their potential advantages such as low cost, light weight and roll-to-roll manufacturing on flexible substrates. In the past two decades, the power conversion efficiency (PCE) of organic-based solar cells has been improved steadily.[1−4] However, it is still low in comparison with inorganic semiconductor counterparts. In general, two major factors that restrict the further enhancement of the PCE are short exciton diffusion length (typically $L_D \sim 10$ nm, much less than the optical absorption length $L_A \sim 100$ nm) and poor charge carrier mobility in most organic semiconductors.[5,6] In order to address the first problem, electron donor and acceptor materials were blended into interpenetrating network structure known as BHJs.[1] In addition, the design of tandem structures, in which multiple organic layers covering complementary absorption spectra are used for enhancing spectral coverage, is another effective approach,[3,6,7] but the complicated fabrication procedure and the demand for the intercellular layer are additional difficulties.

*Project supported by the National Natural Science Foundation of China (Grant Nos. 60978060, 10804006, 10974013 and 10774013), the Research Fund for the Doctoral Program of Higher Education, China (Grant Nos. 20090009110027 and 20070004024), the Research Fund for the Youth Scholars of the Doctoral Program of Higher Education, China (Grant No. 20070004031), the Beijing Nova Program (Grant No. 2007A024)), the Beijing Municipal Natural Science Foundation (Grant No. 1102028), the National Natural Science Funds for Distinguished Young Scholar (Grant No. 60825407), the Beijing Municipal Science & Technology Commission (Grant No. Z090803044009001), and the National Basic Research Program of China (Grant No. 2010CB327705).
†Corresponding author. E-mail: zhengxu@bjtu.edu.cn
‡E-mail: fjzhang@bjtu.edu.cn
© 2010 Chinese Physical Society and IOP Publishing Ltd

Zhang *et al.*[8] reported a simple tandem structure in which a thin CuPc layer was inserted between PEDOT:PSS and P3HT:PCBM layers. Two individual subcells of CuPc/PCBM and P3HT:PCBM were formed and regarded as a parallel connection, resulting in the increased short-circuit current density (J_{sc}) and PCE. Hayashi *et al.*[9] improved the open-circuit voltage (V_{oc}) by incorporating MEH-PPV into P3HT:PCBM BHJ solar cells, and attributed the enhancement to the modification of the HOMO level of the polymer. In the present paper, the influence of a small-molecule material Alq_3 on the performance of polymer solar cells is investigated in devices based on MEH-PPV and PCBM blend. We adopt two approaches, which are simply to dope Alq_3 into MEH-PPV:PCBM solution and to deposit Alq_3 on the top of MEH-PPV:PCBM composite film via thermal evaporation. The improved performance of PSCs is obtained for the devices using Alq_3 as an interlayer between MEH-PPV:PCBM and Al layers.

2. Experimental detail

All the devices were fabricated on patterned indium tin oxide (ITO) coated glass substrates, which had been carefully cleaned by acetone, ethanol and deionized water consecutively and then blown dry by nitrogen gas. After the cleaned ITO substrates were exposed to UV-ozone for 10 min, a thin layer of poly(3,4-ethylenedioxythiophene):poly(styrenesulfonate) (PEDOT:PSS) was spin-coated onto the ITO surface with a speed of 2000 rpm (round per minute) for 50 s and then baked at 120 °C for 10 min. The active layer of MEH-PPV:PCBM (dissolved in chlorobenzene with a weight ratio of 1:4) with and without Alq_3 (dissolved in chloroform) doping were both spin-coated at 2000 rpm. The ratio of Alq_3 to MEH-PPV ranged from 0 to 30 wt.%. Finally, a buffer layer of Alq_3 and an Al cathode were deposited via thermal evaporation through a shadow mask, giving an active device area of 0.1 cm^2. Figure 1 shows the device structure of the polymer solar cells and the molecular structures of the organic materials used in the study.

The current–voltage (I–V) characteristics were measured using a Keithley 2410 source measurement unit in the dark and under illumination of 150 W Xenon lamp with an intensity of 150 mW/cm^2. The absorption (ABS) spectra of organic films spin-coated on pre-cleaned quartz substrates were measured with Shimadzu UV-3101 PC spectrometer and the photoluminescence (PL) spectra were obtained by charge-coupled devices (CCDs). All the measurements were performed under ambient atmosphere at room temperature.

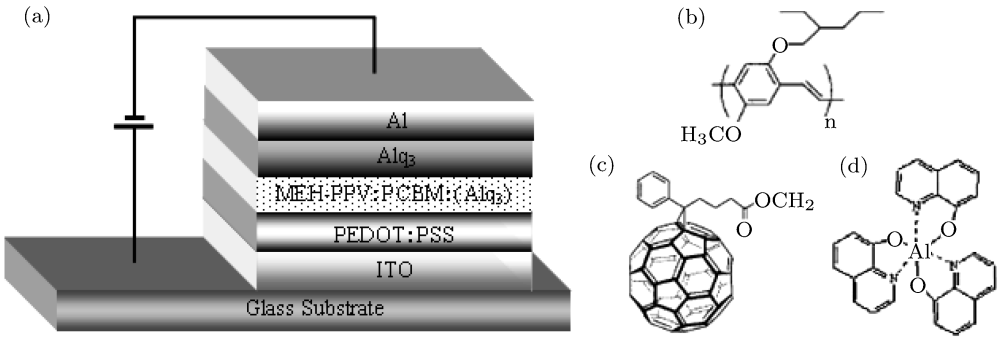


Fig. 1. Device structure of polymer solar cells (a), the chemical structures of MEH-PPV (b), PCBM (c) and Alq_3 (d).

3. Results and discussion

The absorption spectra of MEH-PPV:PCBM (1:4) films with and without Alq_3 doping were measured and are shown in Fig. 2. The main absorption peaks of pure MEH-PPV, PCBM and Alq_3 are located in the vicinities of 500 nm, 335 nm and 395 nm, respectively. The complementary absorption of Alq_3 enhances the light harvesting in a range of 350–450 nm where MEH-PPV and PCBM absorb the light weakly, thereby broadening the absorption spectrum of the whole active layer. Comparing the PL spectrum of Alq_3 with the absorption spectrum of MEH-PPV (see Fig. 3(a)), we find an effective spectral overlap, which indicates a probability of Förster energy transfer from

Alq_3 to MEH-PPV. To further confirm this, the PL spectra of MEH-PPV:Alq_3 with various blend ratios ($1 : x$, $x = 0$, 0.3, 0.6, 1) are shown in Fig. 3(b) (the excitation wavelength was 350 nm). There is no emission of Alq_3 for the 30% doping concentration, suggesting that the energy transfer from Alq_3 to MEH-PPV is nearly absolute. However, when the doping concentration increases to 60%, the emission of Alq_3 peaked at around 530 nm appears, which indicates an incomplete energy transfer; when it further increases to 100%, the Alq_3 emission is more obvious. On varying the excitation wavelength to 390 nm, the same phenomenon was observed (the relevant data are not shown here).

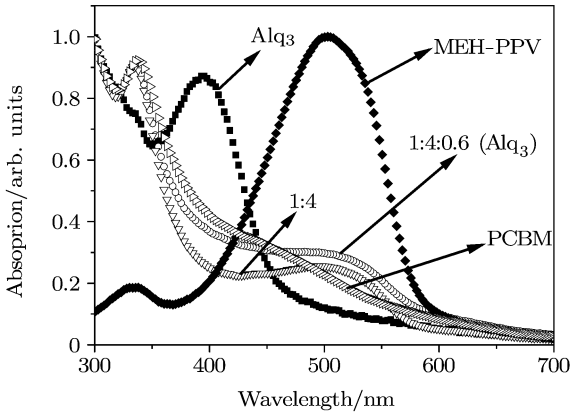


Fig. 2. Normalized absorption spectra of MEH-PPV (solid diamonds), PCBM (open up-triangles), Alq_3 (solid squares), MEH-PPV:PCBM (1:4 in weight) (open down-triangles) and MEH-PPV:PCBM:Alq_3(1:4:0.6 in weight) (open circles) films on quartz substrates.

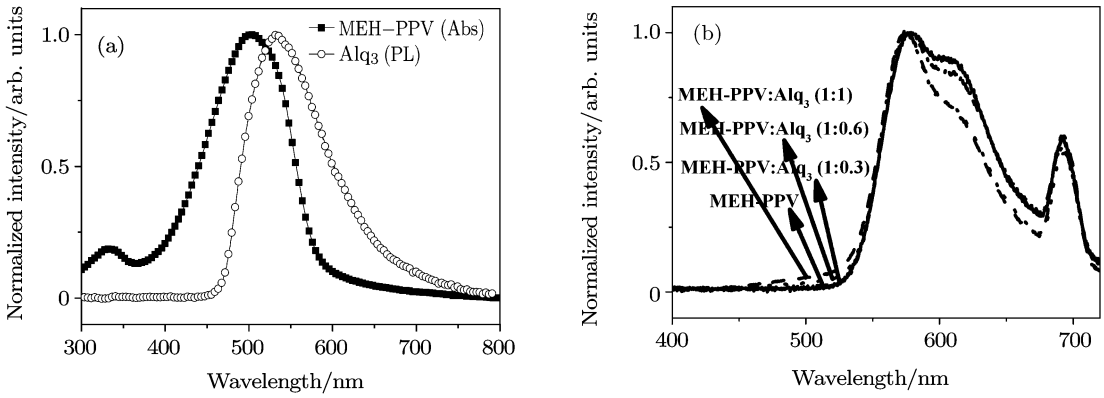


Fig. 3. (a) Optical absorption of MEH-PPV film and PL spectrum of Alq_3 film, and (b) PL spectra of pure MEH-PPV and MEH-PPV:Alq_3 (1:0.3, 1:0.6 and 1:1) films with 350 nm excitation.

3.1. Influence of Alq_3 doping on performances of PSCs

The current density versus voltage (J–V) characteristics of the standard device: ITO/PEDOT:PSS/MEH-PPV:PCBM (1:4 in weight)/Al and 5% Alq_3 doped device: ITO/PEDOT:PSS/MEH-PPV:PCBM:Alq_3 (1:4:5% in weight)/Al under illumination at 150 mW/cm^2 are depicted in Fig. 4. With Alq_3 doping, all photovoltaic performance parameters are descending as compared with those of the undoped device. Comparing the two J–V curves, we find that the doped-device exhibits a higher series resistance (R_s) and a lower parallel resistance (R_p), which may be responsible for the drop of the device performance. The values of R_s and R_p are given by the inverse gradient of the photo J–V curve at 0 mA/cm^2 and at 0 V, respectively. It is known that J_{sc} strongly depends on charge mobility in addition to optical absorption.[10] According to the literature report, the electron mobility of Alq_3 ($\mu_e \sim 10^{-6}$ cm^2·V^{-1}·s^{-1}) is much lower than that of PCBM ($\mu_e \sim 10^{-3}$ cm^2·V^{-1}·s^{-1}), which inevitably results in the increase of the bulk resistance.[11,12] The electron transport is impeded due to a higher R_s, leading to the reduction in J_{sc}. As for the lower fill factor (FF), it is also attributed to the increased R_s and decreased R_p, caused by the low charge carrier mobility of Alq_3.

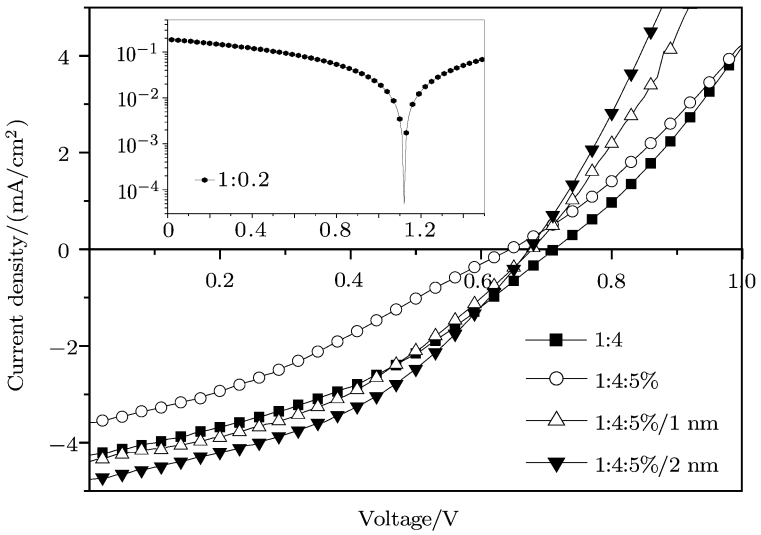


Fig. 4. J–V characteristics of the standard device, only 5% Alq_3-doped device and 5% Alq_3 doped-device modified by 1 nm and 2 nm thermally evaporated Alq_3, respectively. The illumination intensity is 150 mW/cm^2. Insert shows J–V characteristic of MEH-PPV:Alq_3 (1:0.2) under the same illumination.

Table 1. Performance summary of organic photovoltaic devices with Alq_3 doping as well as both Alq_3 doping and modification (1:4:0.5/1 nm (2 nm) represents the 5% Alq_3 doped device with 1 nm (2 nm) thermally evaporated Alq_3 as a buffer layer).

	J_{sc}/(mA/cm^2)	V_{oc}/V	FF/%	PCE/%	R_s/Ω	R_p/Ω
1:4	4.26	0.71	37.9	0.76	857.60	3776.11
1:4:5%	3.58	0.64	32.5	0.50	1168.36	3499.03
1:4:5%/1 nm	4.40	0.68	39.8	0.79	551.07	3700.45
1:4:5%/2 nm	4.76	0.67	42.0	0.89	454.29	4006.61

To thoroughly study the influence of Alq_3 doping on device performance, the doping concentration is varied from 0 to 30% while the MEH-PPV:PCBM ratio (1:4) keeps constant. Figure 5 shows the J–V characteristics for the devices with various Alq_3 doping ratios. As the amount of Alq_3 increases, the J_{sc} decreases from 4.91 mA/cm^2 to 3.86 mA/cm^2, but exhibits a non-monotonic trend; while the V_{oc} reduces from 0.8 V to 0.64 V monotonically. Figure 6 shows the variations of J_{sc}, V_{oc} and FF with Alq_3 doping ratio. For 2% Alq_3 doping, it is worth noting that the FF improves dramatically from 41% to 45.6%. In the MEH-PPV:PCBM system, the hole mobility of MEH-PPV ($\mu_h \sim 10^{-6}$ cm^2·V^{-1}·s^{-1}) is significantly lower than electron mobility of PCBM ($\mu_e \sim 10^{-3}$· cm^2·V^{-1}·s^{-1}).[13] Although it has been found that the hole mobility increases when PCBM is blended into a poly(phenylene vinylene) derivative compared with the pristine polymer films, the mobility difference between electrons and holes in the blend also exists, which results in the limitation of FF.[14] By incorporating Alq_3 into the MEH-PPV:PCBM system, the carrier transport is more balanced due to the decrease of electron mobility to a proper extent. This can prevent the hole accumulation and consequently results in a larger FF. When the doping ratio of Alq_3 is higher than 2%, the FF drops off because of the over decrease of the electron mobility. As the doping ratio of Alq_3 goes up to 10%, the J_{sc} increases from 3.87 mA/cm^2 to 4.35 mA/cm^2 as compared with that of 2% Alq_3-doped device. This can be rationalized in terms of the improved light harvesting caused by the absorption of Alq_3 and the effective energy transfer from Alq_3 to MEH-PPV. However, the J_{sc} is still small compared with that of undoped-device. One possible reason is due to the significantly increased R_s. Another reason is that the excitons cannot be split efficiently at the MEH-PPV/Alq_3 interface,[15] which is testified by the MEH-PPV:Alq_3 (1:0.2) BHJ device yielding the J_{sc} only 0.19 mA/cm^2 (see the insert of Fig. 4). When the doping ratio of Alq_3 reaches up to 30%, the J_{sc} decreases to 3.86 mA/cm^2. As the above discussion, 30% Alq_3 can transfer the energy to MEH-PPV almost absolutely in MEH-PPV:Alq_3

blend film. However, it is known that the energy transfer efficiency is inversely proportional to the sixth power of donor-to-acceptor distance. After blending a large amount of PCBM into MEH-PPV:Alq_3 solution, the distance between Alq_3 molecules and MEH-PPV molecules will be enlarged, which maybe results in the incomplete energy transfer. This is why the J_{sc} decreases for 30% Alq_3-doped device as compared with that of 10% Alq_3-doped device.

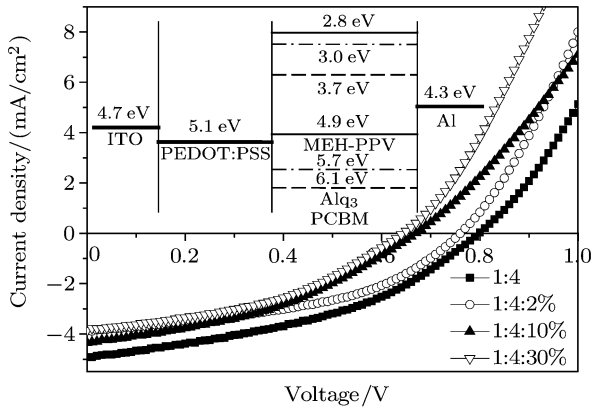


Fig. 5. J–V characteristics for BHJ devices with different Alq_3 doping ratios under illumination. Insert shows schematic energy band diagram of the MEH-PPV:PCBM:Alq_3 BHJ device.

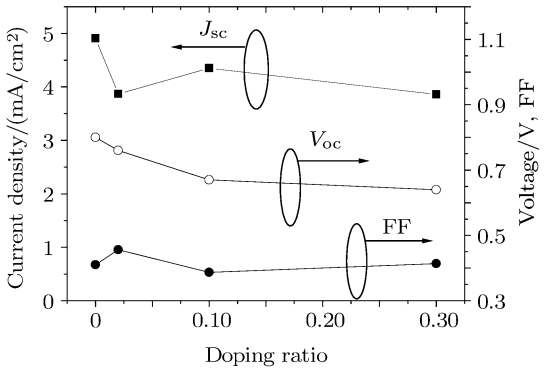


Fig. 6. J_{sc} (■), V_{oc} (◯) and FF (•) of photovoltaic devices each as a function of Alq_3 doping ratio.

The introduction of Alq_3 also affects the value of V_{oc} for MEH-PPV:PCBM solar cells. Up to now, the origin of V_{oc} remains controversial. Most reports suggest that V_{oc} depends mainly on the energy difference between the highest occupied molecular orbital (HOMO) of the donor and the lowest unoccupied molecular orbital (LUMO) of the acceptor.[9,16,17] Besides, it is also influenced by the surface morphology of the polymer thin films[18] and the difference in work function between the two electrodes.[19] Chan *et al.*[20] improved the V_{oc} by doping rubrene into standard CuPc/C_{60} organic photovoltaic device, and attributed the increased V_{oc} to the large energy difference between the HOMO of rubrene and LUMO of C_{60} compared with that between CuPc and C_{60}. A similar conclusion and also a similar interpretation were given by Hayashi *et al.*[9] and Kao *et al.*[16] As shown in the insert of Fig. 5,[9,16] the energy difference between the HOMO of MEH-PPV and LUMO of Alq_3 is also larger than that between MEH-PPV and PCBM, but the V_{oc} of Alq_3 doped-devices is descending rather than ascending as compared with that of undoped-device. As stated above, it is believed that the excitons are generated mainly in MEH-PPV because of the weak absorption of PCBM and the energy transfer from Alq_3 to MEH-PPV which is almost absolute. As a consequence, two individual subcells, namely MEH-PPV:PCBM subcell and MEH-PPV:Alq_3 subcell, are formed and regarded as a parallel connection. The stand-alone MEH-PPV:Alq_3 photovoltaic cell exhibits a V_{oc} of 1.12 V (see the inset in Fig. 4). According to many relevant studies[9,16,20], the V_{oc} of ternary blend solar cell should be intermediate between that of two stand-alone subcells, which is between 0.8 V and 1.12 V herein. However, the experimental results are apparently discrepant with this conclusion. It is well known that V_{oc} is not only dependent on the difference between the energy levels of the donor HOMO and acceptor LUMO, but also influenced by the surface morphology of the active blend films. As a small-molecule material, the very low solubility of Alq_3 may deteriorate the bicontinuous D–A network morphology due to nonuniform distribution throughout the blend film, which probably results in the V_{oc} drop.

3.2. Influence of Alq_3 modification as a buffer layer on performances of PSCs

In order to elucidate the effect of Alq_3 on the MEH-PPV:PCBM (1:4) solar cells, the structure of ITO/PEDOT:PSS/MEH-PPV:PCBM (1:4)/Alq_3/Al was designed, in which Alq_3 was deposited through thermal evaporation and the thickness, ranging from 1 nm to 3 nm, was monitored with a quartz oscillating crystal. The illuminated J–V characteristics of the devices with different thicknesses of Alq_3 are depicted in Fig. 7. After introducing Alq_3 as a buffer layer, all the parameters are improved. At an optimized thickness of 1 nm, the PCE increases by about 80% compared with that of the standard device. Table 2 summarizes the key cell parameters as a function of

Alq_3 thickness under illumination. Song *et al.*[21] supposed that the function of a thin buffer layer for efficiency improvement was to protect the organic layer during metal deposition, which is also supported by other investigations.[22,23] Here, we suggest three other effects: (i) preventing the excitons generated in MEH-PPV from quenching at the polymer/Al interface, (ii) blocking the diffusion of holes from MEH-PPV to Al due to the lower HOMO level of Alq_3 compared with that of MEH-PPV (see Fig. 5 insert),[24] and (iii) increasing the light harvesting, owing to the absorption of Alq_3 and energy transfer from Alq_3 to MEH-PPV. In addition, among the three photovoltaic parameters, we should especially note that the V_{oc} also increases for the devices with Alq_3 as a buffer layer, which indirectly demonstrates that the reduced V_{oc} for Alq_3 doped devices originates from the worsen morphology caused by the low solubility of Alq_3.

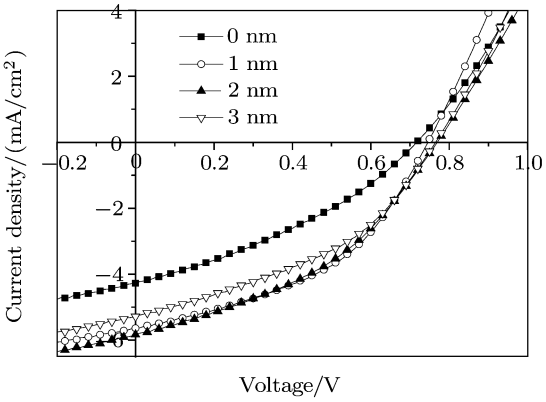


Fig. 7. *J–V* characteristics of the standard device: ITO/PEDOT:PSS/MEH-PPV:PCBM (1:4)/Al and Alq_3 modified device: ITO/PEDOT:PSS/MEH-PPV:PCBM (1:4)/Alq_3 (1, 2 and 3 nm)/Al under illumination.

Table 2. Key parameters for organic photovoltaic devices with different thicknesses of Alq_3 as a buffer layer.

Alq_3/nm	J_{sc}/(mA/cm^2)	V_{oc}/V	FF/%	PCE/%	R_s/Ω	R_p/Ω
0	4.28	0.72	34.0	0.70	672.72	2961.85
1	5.64	0.75	44.2	1.25	397.54	3816.25
2	5.83	0.77	40.2	1.20	529.05	3147.44
3	5.26	0.77	40.5	1.09	484.25	3066.68

3.3. Influence of both Alq_3 doping and modification on performances of PSCs

For the 5% Alq_3 doped device discussed at the beginning, the low PCE as compared with that of the undoped device is ascribed mainly to the increased R_s and the decreased R_p. On the other hand, adopting Alq_3 as a buffer layer can reduce the value of R_s and enhance the value of R_p (see Table 2). With this consideration, we modified the 5% Alq_3 doped device with 1 nm and 2 nm thermally evaporated Alq_3, separately. Their *J–V* characteristics under illumination are shown in Fig. 4. Table 2 listes the key parameters of the photovoltaic devices with Alq_3 doping as well as both Alq_3 doping and modification. After the devices are modified, their parameters are all almost recovered. The values of J_{sc} and FF are even high as compared with those of the standard device, giving a slight enhancement of the PCE despite the improved but still low V_{oc}. Additionally, it can be clearly seen that as expected, the value of R_s of the device with Alq_3 doping and modification decreases and is even lower than that of the standard device. As we know, the R_s is composed of the bulk resistance ($R_{s,bulk}$) of the active layer and the contact resistance ($R_{s,contact}$) between the active layer and the electrodes.[25] Despite the increased $R_{s,bulk}$ caused by the lower carrier mobility for the Alq_3 doping device, the modification with 1 nm (or 2 nm) Alq_3 can compensate this loss by reducing the $R_{s,contact}$, which results in a smaller value of R_s. This further confirms that adopting Alq_3 as a buffer layer is an effective approach to the improvement of the device performances of PSCs.

4. Conclusion

We have investigated the influence of a small-molecule material Alq_3 on the performance of polymer solar cells based on MEH-PPV:PCBM blend via the methods of doping and thermally evaporating Alq_3. For the Alq_3-doped device, the reduced performance may be due to the low carrier mobility and the low solubility of Alq_3, resulting in the increased R_s and the worsen morphology of the active film, despite the

broadened absorption spectrum with considering the energy transfer from Alq_3 to MEH-PPV. On the other hand, all the photovoltaic parameters are improved by adopting Alq_3 as a buffer layer, which can be explained by the increased light absorption, as well as effectively preventing the excitons and holes from diffusing to the Al cathode. We modify the 5% Alq_3-doped device with 1 nm and 2 nm Alq_3 interlayer separately. Their parameters are all almost recovered, yielding a slight enhancement of the PCE as compared with that of the standard device.

References

[1] Yu G, Gao J, Hummelen J C, Wudl F and Heeger A J 1995 *Science* **270** 1789

[2] Reyes-Reyes M, Kim K and Carroll D L 2005 *Appl. Phys. Lett.* **87** 083506

[3] Kim J Y, Lee K, Coates N E, Moses D, Nguyen T Q, Dante M and Heeger A J 2007 *Science* **317** 222

[4] Chen H Y, Hou J H, Zhang S Q, Liang Y Y, Yang G W, Yang Y, Yu L P, Wu Y and Li G 2009 *Nature Photon.* **3** 649

[5] Peumans P, Uchida S and Forrest S R 2003 *Nature* **425** 158

[6] Peumans P, Yakimov A and Forrest S R 2003 *J. Appl. Phys.* **93** 3693

[7] Zhao D W, Sun X W, Jiang C Y, Kyaw A K K, Lo G Q and Kwong D L 2008 *Appl. Phys. Lett.* **93** 083305

[8] Zhang C F, Tong S W, Jiang C Y, Kang E T, Chan D S H and Zhu C X 2008 *Appl. Phys. Lett.* **92** 083310

[9] Hayashi Y, Sakuragi H, Soga T, Alexandrou I and Amaratunga G A J 2008 *Colloids and Surfaces* A **313–314** 422

[10] Zhang F L, Ceder M and Inganäs O 2007 *Adv. Mater.* **19** 1835

[11] Kepler R G, Beeson P M, Jacobs S J, Anderson R A, Sinclair M B, Valencia V S and Cahill P A 1995 *Appl. Phys. Lett.* **66** 3618

[12] Gupta D, Bag M and Narayan K S 2008 *Appl. Phys. Lett.* **92** 093301

[13] Inigo A R, Chiu H C, Fann W, Huang Y S, Jeng U S, Hsu C H, Peng K Y and Chen S A 2003 *Synth. Met.* **139** 581

[14] Mihailetchi V D, Wildeman J and Blom P W M 2005 *Phys. Rev. Lett.* **94** 126602

[15] Liu Y X, Summers M A, Edder C, Fréchet J M J and McGehee M D 2005 *Adv. Mater.* **17** 2960

[16] Kao P C, Chu S Y, Huang H H, Tseng Z L and Chen Y C 2009 *Thin Solid Films* **517** 5301

[17] Scharber M C, Mühlbacher D, Koppe M, Denk P, Waldauf C, Heeger A J and Brabec C J 2006 *Adv. Mater.* **18** 789

[18] Liu J, Shi Y and Yang Y 2001 *Adv. Funct. Mater.* **11** 420

[19] Brabec C J 2004 *Sol. Energy Mater. Sol. Cells* **83** 273

[20] Chan M Y, Lai S L, Fung M K, Lee C S and Lee S T 2007 *Appl. Phys. Lett.* **90** 023504

[21] Song Q L, Li F Y, Yang H, Wu H R, Wang X Z, Zhou W, Zhao J M, Ding X M, Huang C H and Hou X Y 2005 *Chem. Phys. Lett.* **416** 42

[22] Li Y W, Liu P Y, Hou L T and Wu B 2010 *Acta Phys. Sin.* **59** 1248 (in Chinese)

[23] Wang N N, Yu J S, Zang Y and Jiang Y D 2010 *Chin. Phys.* B **19** 038602

[24] Orimo A, Masuda K, Honda S, Benten H, Ito S, Ohkita H and Tsuji H 2010 *Appl. Phys. Lett.* **96** 043305

[25] Aernouts T, Geens W, Poortmans J, Heremans P, Borghs S and Mertens R 2002 *Thin Solid Films* **403–404** 297